International Journal of Solids and Structures 51 (2014) 599–611

Contents lists available at ScienceDirect

International Journal of Solids and Structures

journal homepage: www.elsevier.com/locate/ijsolstr

Liner wrinkling and collapse of bi-material pipe under bending

Lin Yuan, Stelios Kyriakides *

Research Center for Mechanics of Solids, Structures & Materials, WRW 110, The University of Texas at Austin, Austin, TX 78712, United States

ARTICLE INFO

Article history:
Received 20 May 2013
Received in revised form 20 August 2013
Available online 30 October 2013

Keywords:
Lined pipe
Bending
Liner wrinkling
Liner collapse
Plastic buckling

ABSTRACT

Lining internally a carbon steel pipe with a thin layer of corrosion resistant material is an economical method for protecting offshore tubulars from the corrosive ingredients of hydrocarbons. In applications involving severe plastic bending, such as in the reeling installation process, the liner can detach from the outer pipe and develop large amplitude buckles that compromise the flow. This paper outlines a numerical framework for establishing the extent to which lined pipe can be bent before liner collapse. The modeling starts with the simulation of the inflation process through which the two tubes develop interference contact pressure. Bending the composite structure leads to differential ovalization and eventually separation of part of the liner from the outer pipe. The unsupported strip of the liner on the compressed side first wrinkles and at higher curvature buckles and collapses in a diamond shaped mode. The sensitivity of the collapse curvature to the various parameters of the problem is studied, and amongst other findings the onset of collapse is shown to be very sensitive to small geometric imperfections in the liner. It is also demonstrated that bending the pipe under modest amounts of internal pressure can delay liner collapse to curvatures that make it reelable.

1. Introduction

In many offshore applications carbon steel pipe is lined internally with a thin layer of a corrosion resistant material in order to protect it from corrosive ingredients in hydrocarbons it carries during its operation. The most widely used product is assembled by inserting a slightly undersized tubular liner inside the carbon steel pipe and then mechanically expanding both so that the two tubes end up in interference contact with each other (exact steps followed differ to some degree between manufacturers – e.g., Butting Brochure; Rommerskirchen et al. (2003), de Koning et al. (2003), Montague (2004)). In offshore operations the carbon steel pipe carries most of the usual loads of internal and external pressure, tension and bending while the thin liner (2–4 mm) protects the line from corrosive ingredients in the hydrocarbons. However, in cases that involve significant plastic bending of the composite structure, such as in the reeling installation method or in lines susceptible to lateral buckling on the sea floor, the liner can detach from the outer pipe and develop large wrinkles and buckles that compromise the flow. A viable alternative is to use pipe with metallurgically "bonded" liner, commonly known as *clad pipe*, however this comes at a significant increase in cost.

Motivated by this challenge, significant efforts have been undertaken by industrial and academic researchers aimed at establishing the extent to which lined pipe can be safely plastically bent, identifying the main factors that influence liner buckling, and finding ways of delaying it. To this end, several full-scale bending experimental programs have been undertaken during the last several years. Those reported in the open literature include a series of bending results from Gresnigt and co-workers (e.g., Focke (2007), Hilberink et al. (2010, 2011), Hilberink (2011)), bending of heated lined pipe by Cladtek (Montague et al. (2010), Wilmot and Montague (2011)), repeated bending over circular shoes (Tkaczyk et al., 2011), full-scale reeling simulations by Subsea7 and Butting (e.g., Toguyeni and Banse, 2012) and others. Less developed are complementary analytical/numerical efforts reported by the same teams apparently due to the challenges of the problem. The most thorough study of the problem is due to Vasilikis and Karamanos who used FEs to analyze lined pipe under pure bending. They first considered the purely linearly elastic version of the problem (Vasilikis and Karamanos, 2010) and more recently (2012) the more realistic elastic–plastic version (See also recent results in Yuan and Kyriakides, 2013).

Collectively these efforts have contributed to the following state of current understanding of the problem. Bending to curvature levels that correspond to those seen by reeled pipe results in significant plastic deformation of both the carrier pipe and liner. Concurrently the composite structure develops Brazier-type (1927) ovalization of its cross section. This in turn can result in loss of contact and partial separation of the liner from the steel pipe. At some level of deformation, the separated section of the liner buckles into a wrinkling mode, commonly seen in pure bending of single pipe (e.g., see Ju and Kyriakides (1991, 1992), Corona et al. (2006), Kyriakides and Corona (2007), Limam et al. (2010)). As is

* Corresponding author. Tel.: +1 512 471 4167.
E-mail address: skk@mail.utexas.edu (S. Kyriakides).

0020-7683/$ - see front matter © 2013 Elsevier Ltd. All rights reserved.
http://dx.doi.org/10.1016/j.ijsolstr.2013.10.026

common to plastic buckling of shells, wrinkling is followed by a second instability that leads to collapse of the liner in a diamond-type buckling mode (e.g., see references above and for the related plastic buckling under axial load see Tvergaard (1983), Yun and Kyriakides (1990), Kyriakides et al. (2005), Bardi and Kyriakides (2006), Bardi et al. (2006), Kyriakides and Corona (2007)).

The aim of this study is through numerical modeling to add clarity to the sequence of events that lead to liner failure, understand the major factors that influence it, and evaluate several of the methods for delaying failure that are being considered. The main expansion processes through which today's lined pipe is manufactured involve a certain amount of cold forming. This introduces changes to the mechanical properties of the two constituents, leaves behind residual stresses as well as the interference contact stress. Invariably, these changes influence the liner instabilities but to date have been mostly neglected as they tend to complicate the modeling. In the present effort this will be corrected by first simulating the mechanical expansion thus locking in the initial state. Expanded models are subsequently bent taking the structure first through liner separation from the carrier pipe, liner wrinkling, and finally liner localized collapse. The models developed will be used to study these aspects parametrically.

2. Modeling

2.1. Manufacture of lined pipe

Lined pipe consists of a carbon steel carrier pipe with a thin inner layer of corrosion resistant alloy liner. The two tubes are typically expanded together using one of several methods currently in the market, come into contact and remain so after unloading (e.g., Butting Brochure; Rommerskirchen et al. (2003), de Koning et al. (2003), Montague (2004)). The objective is that the finished bi-layer composite ends with some interference contact pressure between the two components (often called "mechanical bonding"). The products in the market today have significant similarities but also some differences. In this study we will concentrate on the expansion process followed by Butting.

For 4–16-inch products the carrier pipe is seamless and is produced by the *plug* or *mandrel* piercing processes (e.g., see Ch. 3 Kyriakides and Corona, 2007). The 2–4 mm corrosion resistant liner (e.g., SS321, SS316L, alloy 625, alloy 825) is most often formed into a continuous longitudinally welded tube from coil. Special care is given to the metallurgical quality and integrity of the weld while also shaping its outer surface to conform to the circular shape of the steel pipe. The finished tube, cut to approximately 12 m length, is placed inside the carrier pipe whose inner surface is previously sandblasted and cleaned. A small gap (g_o) is allowed between the two pipes for ease of insertion. The two concentric pipes are then enclosed inside two semi-circular stiff dies with an ID that will result in the required final diameter of the composite (image ⓪ in Fig. 1). Hydraulic pressure is then applied to the liner causing it to expand and come into contact with the steel pipe as shown in image ①. The pressure is further increased expanding both pipes until the outer surface comes into contact with the stiff die as shown in ②. The pressure is then released causing both pipes to contract. The higher yield stress steel pipe tends to spring back more than the stainless steel liner and this results in interference contact between the two as shown in image ③.

The process was modeled both analytically and numerically treating the system as axisymmetric. Fig. 2 shows results from the FE model based on the parameters of what we designate as the *base case* given in Table 1. Fig. 2a shows the calculated pressure-radial displacement (P-w) response. Here the pressure is normalized by the yield pressure of the steel pipe, P_o, based on its yield stress and final dimensions; the radial displacement of the liner, w, is normalized by the initial gap g_o. Thus, between ⓪

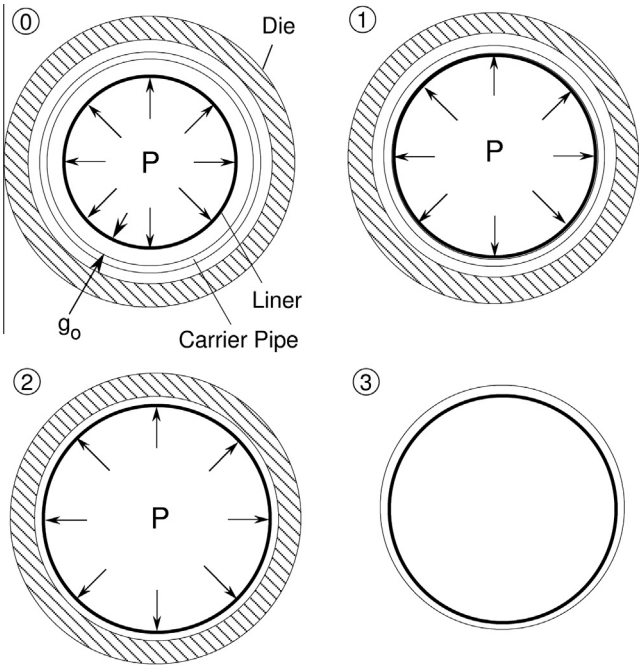

Fig. 1. Schematic representation of the expansion process through which lined pipe is manufactured (Butting brochure).

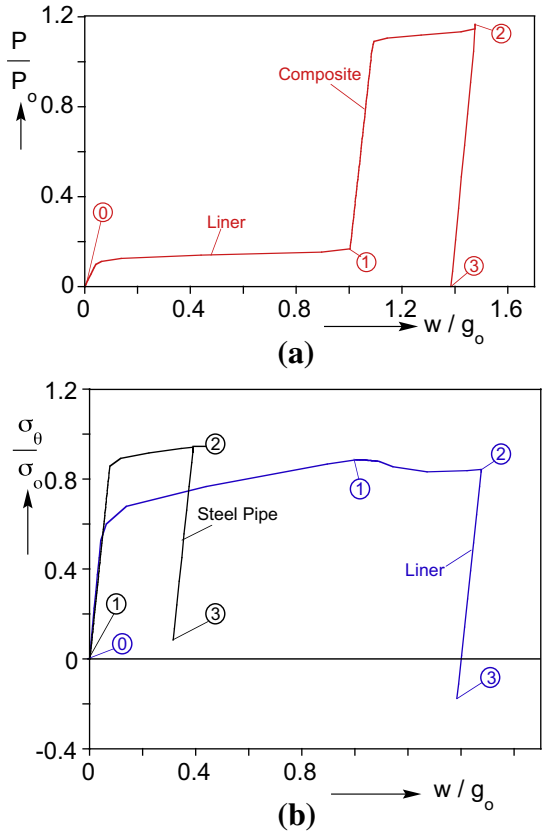

Fig. 2. (a) Pressure-radial displacement response of bi-material structure during hydraulic expansion and (b) corresponding stresses-displacement responses.

Table 1
Main geometric and material parameters of base case.

	D in[a] (mm)	t in[a] (mm)	E Msi[b] (GPa)	σ_o ksi[b] (MPa)
Steel carrier X65	12.75 (323.9)	0.705 (17.9)	30.0 (207)	65.0 (448)
Liner alloy 825	11.34 (288.0)	0.118 (3.0)	28.7 (198)	40.0 (276)

[a] Finish dimensions,
[b] Nominal values.

and ① the liner expands initially elastically and subsequently plastically. It comes into contact with the steel pipe at ① and consequently the response stiffens significantly. The pressure experiences a sharp increase until the steel pipe yields. The two pipes are then plastically expanded further until the carrier comes into contact with the stiff outer die at ②. Subsequently the pressure is gradually removed (③).

Fig. 2b shows the hoop stresses developed in the two pipes during the expansion (both normalized by the yield stress of the steel carrier σ_o). (Note that the loading is biaxial as some axial compression proportional to the pressure is applied simultaneously.) Between ⓪ and ① the liner is expanding freely. Between ① and ② the two are expanding together and this is responsible for the small dip in the liner stress. Finally, the structures unload elastically to ③ with both of them ending up with residual stresses due to a residual interference. The stress is tensile in the steel pipe and compressive in the liner. This is primarily due to the difference in the stress level that each component unloads from, which is quite obvious in Fig. 2b. Other factors that affect the extent of the interference stress will be discussed in the parametric study section.

2.2. Finite element models

As mentioned in the introduction, the problem of interest undergoes several stages. Thus, it is discretized using several levels of FE models each adapted to the challenges of each stage. The primary model involves a section of the composite pipe of length $2L$, outer diameter D, and carrier and liner wall thicknesses of t and t_L respectively. The pipe is bent under pure bending as shown in Fig. 3. For numerical efficiency, symmetry about the mid-span is assumed (plane y–z) as well as about the plane of bending x–z. The steel carrier is meshed with linear 3D elements (C3D8) and the contacting liner with linear shell elements (S4). Unless otherwise stated, the half length of the model will be $L = 20\lambda$, where λ is the half wavelength of an initial axisymmetric geometric imperfection that will be commonly introduced to the liner. Although actual wrinkle wavelengths under inelastic bending can differ to some degree, the value corresponding to elastic buckling of a circular cylindrical shell under uniform compression given below can be viewed as representative (see Ju and Kyriakides (1991, 1992), Corona et al. (2006), Kyriakides et al. (2005), Kyriakides and Corona (2007)).

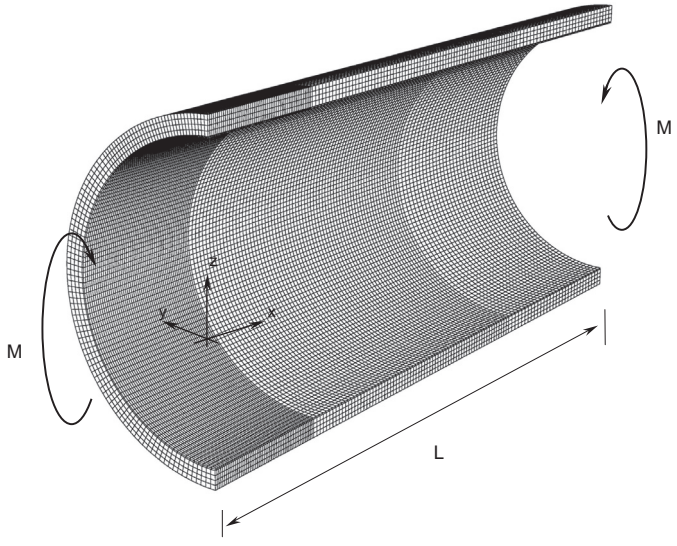

Fig. 3. FE mesh of composite pipe under bending.

$$\lambda = \frac{\pi\sqrt{R_L t_L}}{[12(1-\nu^2)]^{1/4}} \tag{1}$$

where R_L is the mid-surface radius of the liner and ν its Poisson's ratio.

The carrier pipe has four elements through the thickness and both tubes are assigned 108 elements around the half circumference. Most calculations will involve the introduction of small initial geometric imperfections to the liner with a bias towards the mid-span. The bias is introduced in anticipation of the expected localization of buckling and collapse, and in order to accommodate the conduct of systematic parametric studies. Accordingly, axially the mesh has three densities as follows:

$$\{0 \leqslant x \leqslant 4\lambda, 56 \text{ elements}\},$$

$$\{4\lambda \leqslant x \leqslant 14\lambda, 70 \text{ elements}\},$$

$$\{14\lambda \leqslant x \leqslant 20\lambda, 30 \text{ elements}\}.$$

The first plastic instability that develops in circular cylindrical shells under bending is wrinkling of the compressed side (Ju and Kyriakides, 1991). Depending on the D/t of the shell, this is followed by a second bifurcation into a diamond-type buckling mode that leads to localization and collapse (Ju and Kyriakides (1992), Corona et al. (2006), Kyriakides and Corona (2007)). Not surprisingly, initial wrinkling and diamond-type buckling of the liner have been reported in the Delft experiments (e.g., Hilberink et al. (2010, 2011)). Motivated by this, we introduce to the liner two types of initial imperfections, an axisymmetric one with wavelength λ, shown in Fig. 4a, and a non-axisymmetric one with axial wavelength 2λ and m circumferential waves shown in Fig. 4b (Koiter, 1963). The two are combined as shown in Eq. (2) and are modulated by an axially decaying function in order to facilitate localization in the neighborhood of the y–z plane of symmetry

$$\bar{w} = t_L\left[\omega_o \cos\frac{\pi x}{\lambda} + \omega_m \cos\frac{\pi x}{2\lambda}\cos m\theta\right] 0.01^{(x/N\lambda)^2}. \tag{2}$$

Contact between the two layers plays an important role in the problem. The finite sliding option of ABAQUS is adopted with the carrier pipe as the master surface and the liner as the slave surface. Contact is assumed to be frictionless.

As mentioned in Section 2.1, the initial mechanical expansion that brings the two pipes in contact introduces changes to the mechanical properties and leaves behind residual stresses as well as a certain interference pressure. Collectively, these initial conditions of the two materials and structures influence the mechanical behavior of the composite pipe and consequently must be incorporated in the model. Although the most direct approach is to simulate the manufacturing process using the full FE model, the requirement to have liner geometric imperfections with controllable shapes and amplitudes dictated an alternate approach. The manufacturing process was analyzed separately using an axisymmetric model in which the liner is modeled as a shell and the carrier pipe as a solid each with a similar through-thickness

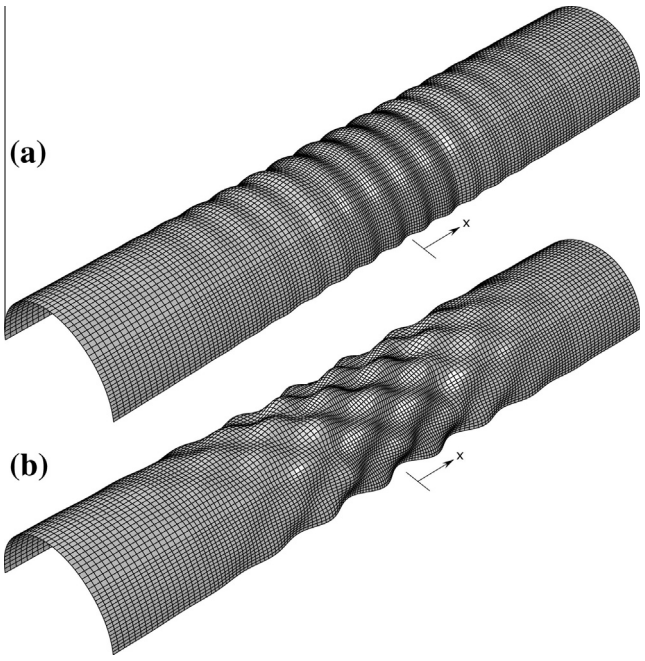

Fig. 4. (a) axisymmetric and (b) non-axisymmetric imperfections adopted.

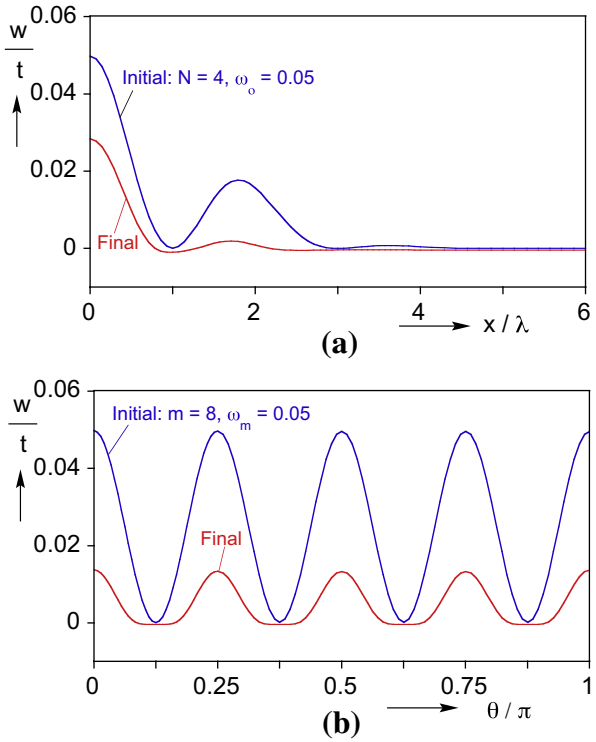

Fig. 5. Comparison of profiles of imperfections initially and after application of manufacturing stress field: (a) axial and (b) circumferential ($x = 0$) profile.

distribution of elements, or integration points, as those of the full model. At the end of the process (point ③ in Figs. 1 and 2) the state of stress and strain in each of the four axisymmetric elements are averaged and the state of stress, the plastic strains, and the equivalent plastic strains are transferred to the nodes and integration points to all through-thickness elements of the full model. The state of stress in the liner is essentially the same through all integration points and is transferred as such to all elements of the liner in the full model. In the process, the two pipes deform slightly, contact pressure develops, and most importantly, the imperfection amplitude is reduced. The veracity of this scheme was evaluated by comparing the stress and deformation states induced by the expansion process using the axisymmetric model and the full 3D model. Such comparisons found the two sets of results to be very close to each other. We note that this can only be done for the perfect geometry case as initial imperfections of the type adopted are essentially erased if exposed to the expansion process.

As reported, in the process of transferring the initial state of stress to the full model the initial imperfection deforms and its amplitude is reduced. Fig. 5 shows comparisons of the initial and final imperfections for $\omega_o = \omega_m = 0.05$ and $N = 4$. Fig. 5a shows the amplitude of the axisymmetric imperfection at mid-span to have been reduced by nearly 50% by the expansion process. Fig. 5b shows the amplitude of the non-axisymmetric imperfection at mid-span for $m = 8$ to have been reduced by nearly 60% and the contact with the outer pipe to have increased. In all calculations involving the base case (Table 1), the models will be assigned the same prehistory due to the expansion. For consistency, the imperfection amplitudes that will be quoted are the initial values.

3. Results

3.1. Wrinkling of perfect structure

As is well established, in the case of single tubes and pipes, plastic bending leads to ovalization of the tube cross section and at some stage to buckling in the form of periodic wrinkling on the compressed side of the structure. The wrinkles have small amplitudes at first appearance, but their amplitudes gradually grow with curvature contributing to some reduction in the stiffness of the response. At some higher level of curvature, the structure develops a second instability that is usually catastrophic. For higher D/t tubes, like those of the liners under consideration here, the second instability is non-axisymmetric buckling (see Chapter 8 of Kyriakides and Corona (2007) for more details).

The onset of plastic bifurcations is best established by using deformation theory instantaneous moduli. Indeed, the procedure we recommend is to use flow theory for non-trivial prebuckling calculations and deformation theory for bifurcation checks––using the state of stress from the flow theory (see Chapter 13 Kyriakides and Corona (2007)). Unfortunately, following this guideline in the present case is complicated by the expansion prehistory and the other nonlinearities of the problem and thus will not be followed. Consequently, we will demonstrate the onset of wrinkling for the base case parameters using flow theory instead, realizing that the actual bifurcation occurs at a lower curvature. (It is noteworthy that Peek and Hilberink (2013) established the onset of bifurcation of a lined cylinder without initial prehistory under axial compression for the case where the two components are of the same material––see also Shrivastava (2010)).

Fig. 6a shows the calculated moment–curvature (M–κ) responses corresponding to the perfect base case where the normalizing variables are based on the parameters of the outer pipe as follows:

$$M_o = \sigma_o D_o^2 t, \quad \kappa_1 = t/D_o^2, \quad D_o = D - t.$$

Shown in the plot are the responses for the composite structure and of the individual steel and liner pipes. Included is the ovalization induced to the liner represented by the change in its diameter $\Delta D/D|_L$. Fig. 6b shows a set of liner deformed configurations with color contours corresponding to the contact pressure between it and the outer tube. The images correspond to the numbered points marked on

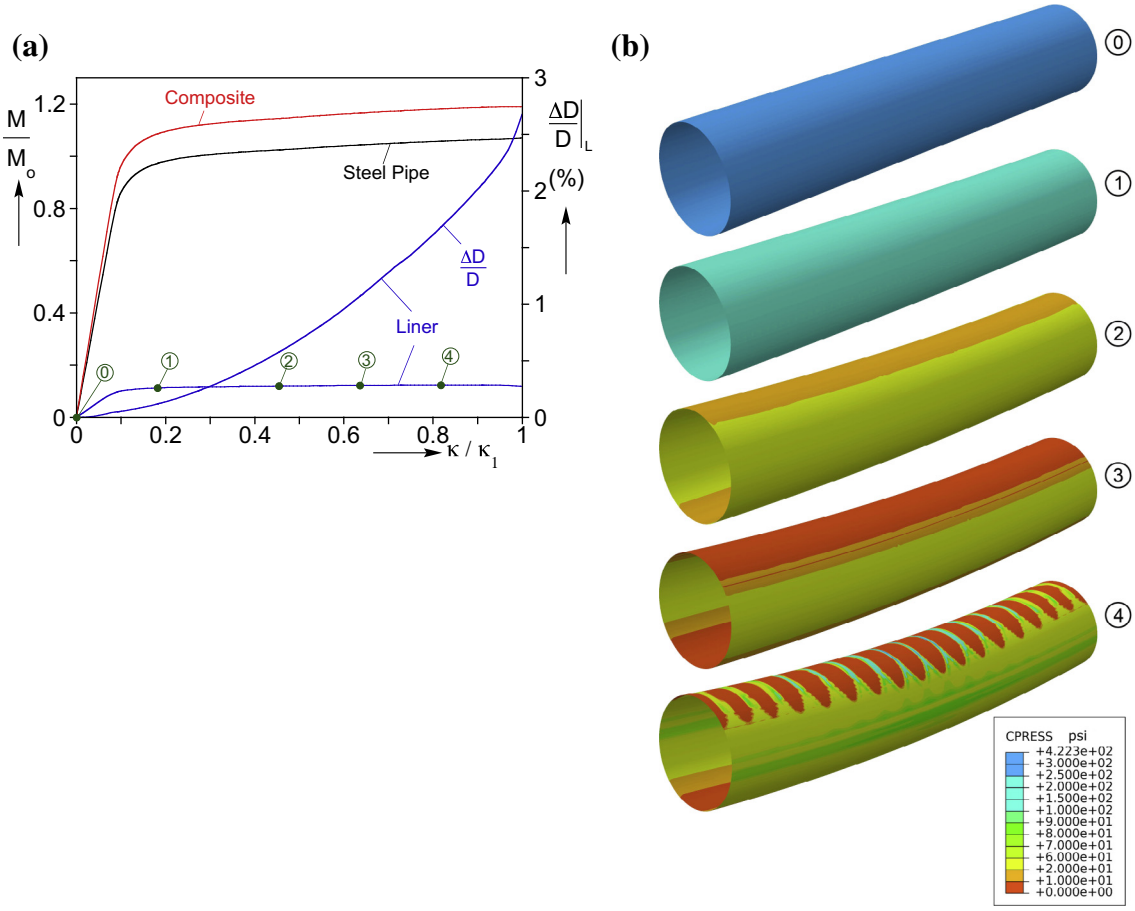

Fig. 6. (a) Base case moment- and ovalization-curvature responses. (b) Liner deformed configurations with superimposed contours of liner contact pressure; correspond to numbered bullets on liner response in Fig. 6a.

the liner response in Fig. 6a. In this case, the expansion process resulted in a contact pressure of about 270 psi (1.86 MPa). Bending plasticizes and ovalizes both tubes and the combined effect leads to a reduction in the contact pressure as illustrated in ①. At higher curvatures, the ovalization of the liner overtakes that of the steel tube (②) eventually causing loss of contact at the two extremes of the cross section as shown in ③. At a curvature of about 0.63 κ_1, the long unsupported section of the liner that is under compression buckles into the periodic wrinkling mode seen at a more developed stage in image ④ (see also Vasilikis and Karamanos, 2012). The amplitude of the wrinkles grows with curvature eventually inducing a second diamond-type buckling mode not shown here. Although this sequence of events is representative of the actual behavior, the curvature at the onset of wrinkling predicted with flow theory is artificially high due to the well-known deformation-flow theory paradox (see Kyriakides and Corona, 2007). A more appropriate bifurcation study of lined pipe under pure bending will be addressed elsewhere.

Manufactured lined pipe is characterized by small geometric imperfections (for cross sectional shape and inner surface imperfections in seamless tubes see §4.5 of Kyriakides and Corona, 2007). Thus, in the remainder of the paper we consider bending of lined pipe with initial liner imperfections.

3.2. Wrinkling and collapse of an imperfect liner

We now consider a lined pipe with the same geometry and material properties, manufactured in a similar manner but with a liner that has small initial imperfections of the type described by Eq. (2) where the value of λ is calculated as in Eq. (1) and $m = 8$ (the effect of these choices will be discussed subsequently). The amplitudes of the imperfections ω_o and ω_m used are listed in the figures; they represent the values prior to expansion. Fig. 7a shows the calculated moment–curvature responses of the composite structure and the individual tubes. Fig. 7b shows a corresponding plot of the detachment, $\delta(0)$, of the compressed generator of the liner in the plane of bending at $x = 0$. Fig. 8a shows two sets of deformed configurations corresponding to the solid bullets marked on the liner responses in Fig. 7. The three moment–curvature responses follow the same trends as those of the perfect geometry case, but in the neighborhood of ② the axisymmetric imperfection is excited and small amplitude wrinkles develop in the central part of liner (see corresponding images ② in Fig. 8a where the color contours represent the magnitude of the separation of the liner from the carrier pipe depicted as Δw.) The amplitude of the wrinkles grows as illustrated in configurations ③ and ④ and so does the separation of the liner from the outer tube. This reduces the bending rigidity of the liner causing the development of a moment maximum at $\kappa = 0.623\kappa_1$ (marked in Fig. 7a with a caret "^"). This is a sign that wrinkling is starting to localize while simultaneously the non-axisymmetric component of the imperfection is excited. The switch to the diamond-type of mode, seen in configurations ⑤, causes an abrupt increase in local separation of the liner from the outer pipe, $\delta(0)$. At higher curvatures, the diamond buckles become more prominent as seen in configurations ⑥ and ⑦ (note the different color scale). A three-dimensional rendering of the buckled liner at a curvature of $\kappa = \kappa_1$ is shown in Fig. 8b. The significant amplitude of the buckles can render this structure non-operational.

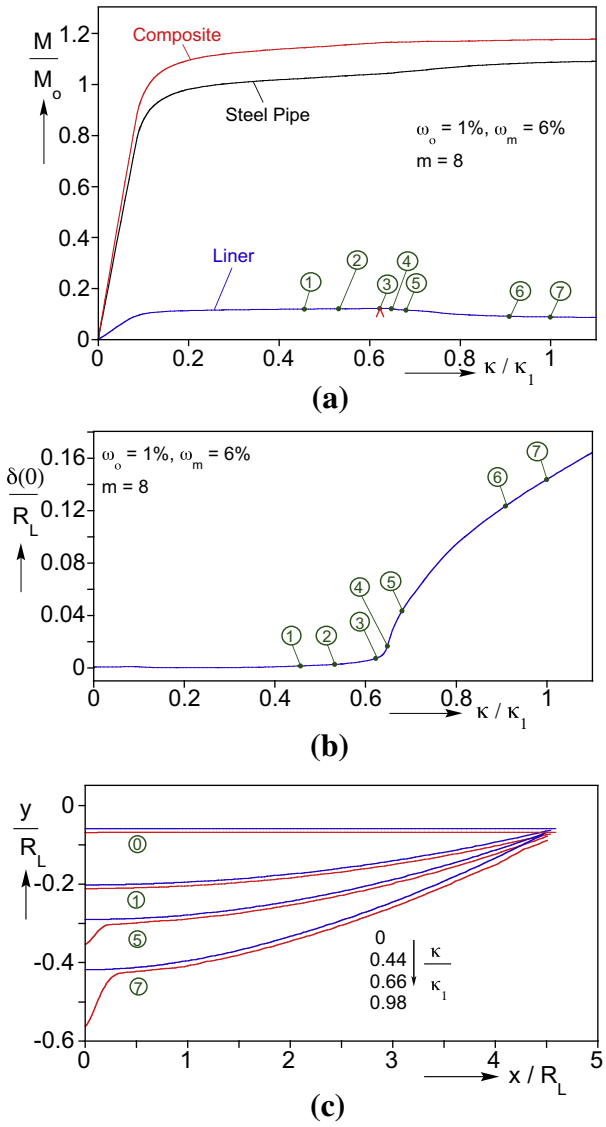

Fig. 7. Imperfect base case responses: (a) moment–curvature, (b) maximum detachment-curvature and (c) axial profiles of compressed generators of outer pipe and liner.

Another view of the localization that takes place is presented in Fig. 7c, which shows the compressed generators of the outer pipe and liner in the plane of bending at different degrees of deformation. The separation of the liner from the outer pipe near the center of the model in contours ⑤ and ⑦ is quite obvious.

We will define the curvature at the moment maximum and the sharp upswing in the separation between the two tubes as the critical collapse curvature. It is reassuring that this sequence of events as well as the collapse mode in images ⑦ in Fig. 8 are qualitatively in good agreement with results from full-scale bending experiments reported in Hilberink et al. (2010, 2011) and Hilberink (2011).

3.3. Imperfection sensitivity of liner collapse

Information on actual liner imperfections introduced during the manufacture of the two tubes and the composite structure at the present are scarce. Consequently the values of the imperfection amplitudes ω_o and ω_m used in the calculations described in Section 3.2 are somewhat arbitrary. In order to better understand the effect of these imperfections on liner collapse, the two amplitudes are varied while keeping the outer pipe and liner geometry and material properties the same as those in Table 1. Fig. 9 shows sets of moment- and maximum detachment-curvature responses for various values of ω_o and fixed values of ω_m and m. Associating again the curvature at the moment maximum and the corresponding point at which the liner detachment experiences significant sudden growth with collapse, it is clear that collapse is extremely sensitive to this imperfection. This point is further highlighted realizing that $0.02t_L$, i.e., the axisymmetric imperfection amplitude before expansion, corresponds to 0.06 mm, a value that is significantly smaller than typical internal surface imperfections left behind by the manufacture of the seamless carrier pipe. Furthermore, we reiterate that this amplitude is reduced by about 50% by the expansion process.

The amplitude of ω_m was also varied keeping ω_o and m constant. Fig. 10 shows similar sets of results for $0 \leqslant \omega_m \leqslant 0.06$. Although these values are somewhat larger that those of ω_o in Fig. 9, it is clear that collapse is sensitive to non-axisymmetric imperfections also. The two sets of results in Figs. 9 and 10 are summarized in Fig. 11 where the liner collapse curvature, κ_{CO}, is plotted against the two imperfection amplitudes. The results demonstrate that although the onset of collapse is sensitive to both types of imperfections, it is much more sensitive to axisymmetric ones.

The mode of the non-axisymmetric imperfection was also considered by varying the value of m adopted in Eq. (2). Fig. 12 shows moment- and maximum detachment-curvature responses of the liner for three values of m from calculations based on the base case parameters (Table 1) and for fixed values of imperfection amplitudes. The results show that collapse is relatively insensitive to the value of m adopted. A careful evaluation of this conclusion revealed that it is valid provided the imperfection amplitudes after expansion have similar values, as was the case for $m = 6$, 8 and 10. It was observed that for $m < 6$ the initial values of ω_o and ω_m had to be smaller in order to end up with similar final imperfection amplitudes after expansion.

In the calculations thus far the value of the half wavelength of the axisymmetric imperfections used corresponded to the elastic value, λ_e, as defined in Eq. (1). A more accurate value can only come from plastic bifurcation values of the composite pipe under bending. Lacking this at the present, we vary λ within reasonable limits using the base case parameters and constant values of imperfections amplitudes. Fig. 13 shows the collapse curvature of the liner to be quite insensitive to the value of λ adopted within the chosen range.

Summarizing the results of this imperfection sensitivity study, it is clear that liner collapse is very sensitive to small initial geometric imperfections left in the liner from the manufacturing process. Furthermore, the outer pipe has been assumed to be perfectly circular and to have uniform thickness, assumptions that require revisiting. In view of the observed significant sensitivity, it is recommended that industry seek to develop methods to quantify imperfections in the initial carrier pipe and in the final lined product, and to the extent possible, tie them to the appropriate manufacturing steps in order to encourage efforts to reduce them.

4. Parametric study

Thus far we have limited attention to a base case that involves a 12-inch outer pipe with $D/t \approx 18$ and a corrosion resistant liner 3 mm thick. In this section we present results from a wider parametric study in which various additional factors that can influence the collapse of liners are examined.

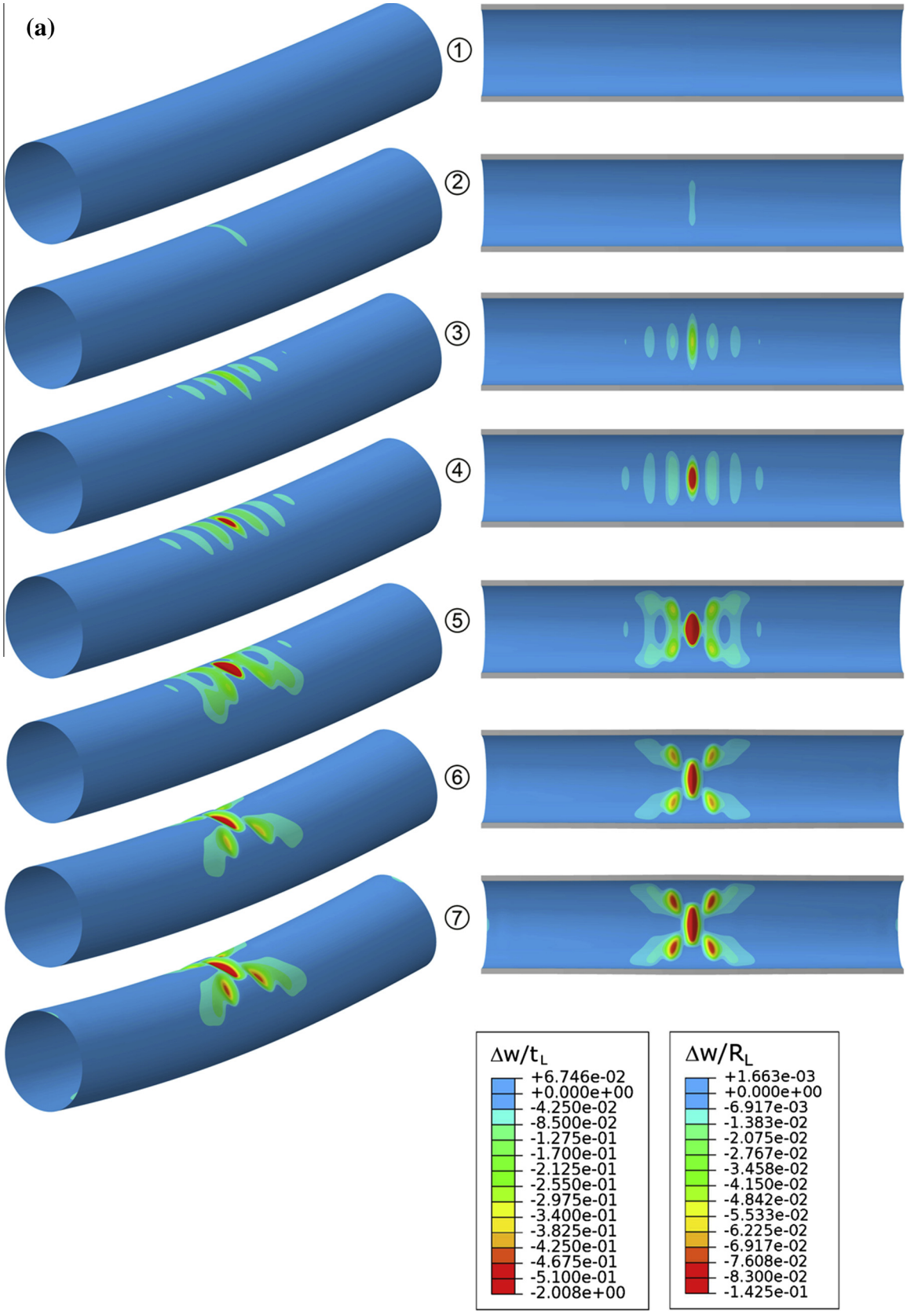

Fig. 8. (a) Sequences of liner deformed configurations showing evolution of wrinkling corresponding to numbered bullets on response in Fig. 7a. On the left are 3D renderings and on the right cross sectional views of compressed side (for images ⑥ and ⑦ use. $\Delta w/R_L$ color scale). (b) Three-dimensional rendering of the buckled liner.

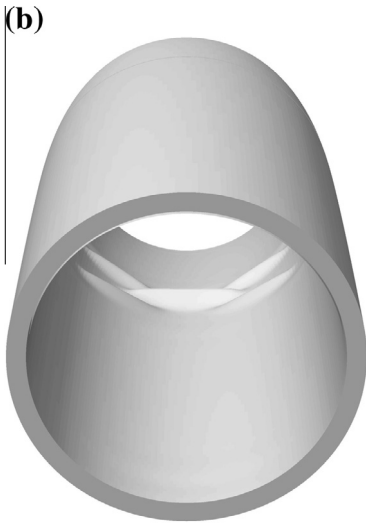

Fig. 8 *(Continued).*

4.1. Pipe diameter

We first consider composite systems of four different steel pipe diameters but keep the D/t at approximately 18.0. In addition, the liner thickness is kept at 3 mm and the material properties of both tubes are kept the same as those used in the base case. Each composite system is assigned similar imperfections (Eq. (2)) and then appropriately expanded as described in Section 2.1. In each case the imperfection half-wavelength λ is determined from Eq. (1) while $m = 8$. Due to the difference in pipe diameter, the expansion process alters the initial imperfections to differing degrees. Thus, for a more systematic comparison of their effect on liner collapse, the amplitudes of the two imperfections were varied so that after expansion the maximum value of $\bar{w}/R_L$ was approximately the same for all four cases, 0.778×10^{-3}.

The models were purely bent and the response of the two-pipe systems was recorded. The results are summarized in Fig. 14, which shows plots of the liner moment- and maximum detachment-curvature responses for outer pipes with diameters of 8.625, 10.75, 12.75 and 14.0 in (designated in the figure as 8, 10, 12, 14 in). In these plots the normalizing variables are as follows: $\kappa_{1b} = t/D_o^2|_b$, $M_{ob} = \sigma_o D_o^2 t|_b$, where the subscript "$b$" implies the variables of the base case, in other words those of the 12-inch pipe system in Table 1. With this normalization the moment and curvature appear in their natural order.

As expected, as the diameter of the pipe increases the moment carried by the liner increases. The behavior of the liner is similar to that described in Figs. 7 and 8: bending causes the liner to separate from the outer pipe; it develops periodic wrinkles the amplitude of which gradually grows, and at some point the non-axisymmetric imperfection is excited enough to lead to the collapse of the liner. Collapse is associated with the moment maxima in Fig. 14a and with the sharp upswing of the detachment variable $\delta(0)$ in Fig. 14b. Clearly, as the pipe diameter decreases the composite pipe can be bent to a larger curvature before the liner collapses. This is caused by the fact that as D decreases so does R_L/t_L while the axial stress induced to the liner by bending decreases.

4.2. Initial gap between carrier and liner tubes

In the manufacturing process that has been simulated in this work outlined in Section 2.1, the liner tube initial diameter is chosen to be somewhat smaller than that of the outer pipe for ease of insertion. In this section we examine the effect of the initial annular gap between the two pipes, g_o, on the collapse of the liner. To this end we simulate the manufacture of the base case system (Table 1) again but start with somewhat different liner initial diameters so that the initial gap varies. Fig. 15 shows the normalized hoop stresses in the steel outer pipe and in the liner plotted against the radial displacement, w/g_{ob}, for four values of g_o: {0.5, 1, 1.5, 2} g_{ob}, where g_{ob} is the value used in the base case calculations in Fig. 2. As the gap increases, the liner has to deform more in order to come into contact with the outer pipe becoming increasingly plasticized. The maximum stress in each liner

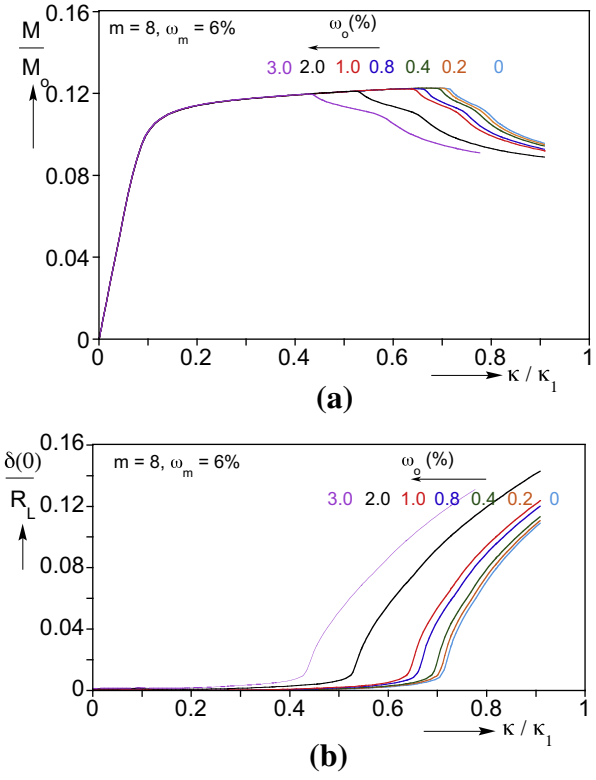

Fig. 9. Effect of axisymmetric imperfection amplitude on liner response. (a) Moment–curvature and (b) maximum detachment-curvature responses.

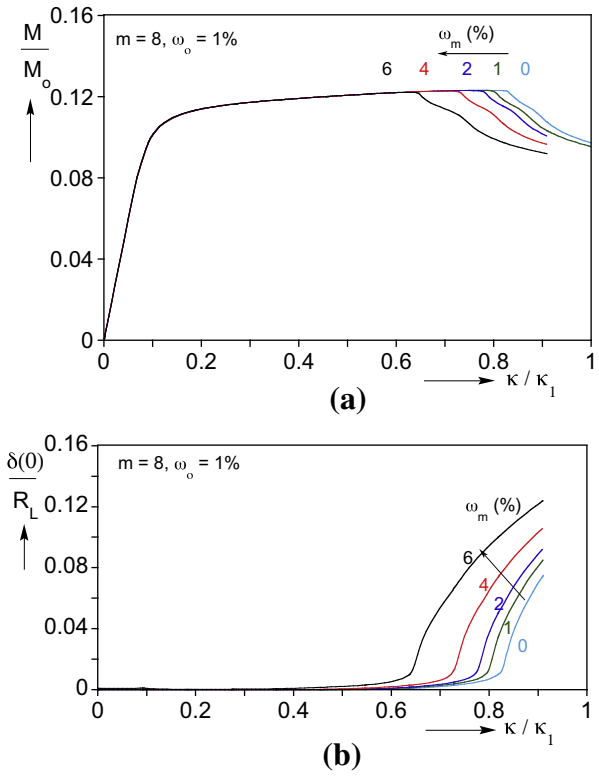

Fig. 10. Effect of non-axisymmetric imperfection amplitude on liner response. (a) Moment–curvature and (b) maximum detachment-curvature responses.

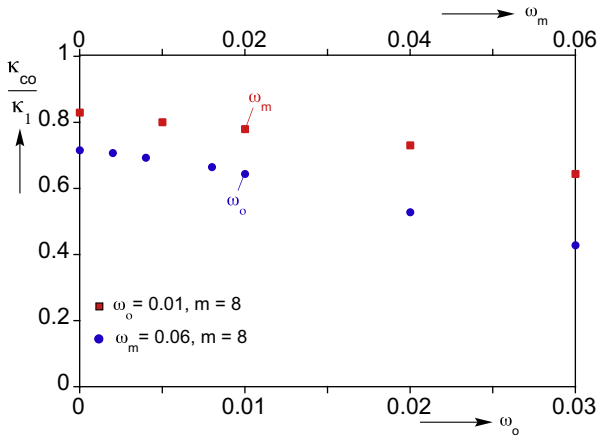

Fig. 11. Collapse curvature sensitivity to axisymmetric (ω_o) and non-axisymmetric (ω_m) imperfection amplitudes.

response corresponds to first contact with the outer pipe and the subsequent lower stress section to simultaneous expansion of the two tubes. The residual hoop stresses left in the two tubes on removal of the pressure are seen to decrease as g_o increases. These residual stresses are of course directly related to the residual contact stress between the two tubes.Because the annular gap influences the contact stress that develops between the two tubes, the final value of a chosen initial liner imperfection depends on g_o. Since it is desirable that the amplitudes of the imperfections of the four cases studied be nearly the same, the initial values of ω_o and ω_m were varied so that the final amplitude of the imperfections was 0.0255 t_L for all four cases. Fig. 16 shows results from bending calculations on each of the four composite tubes.

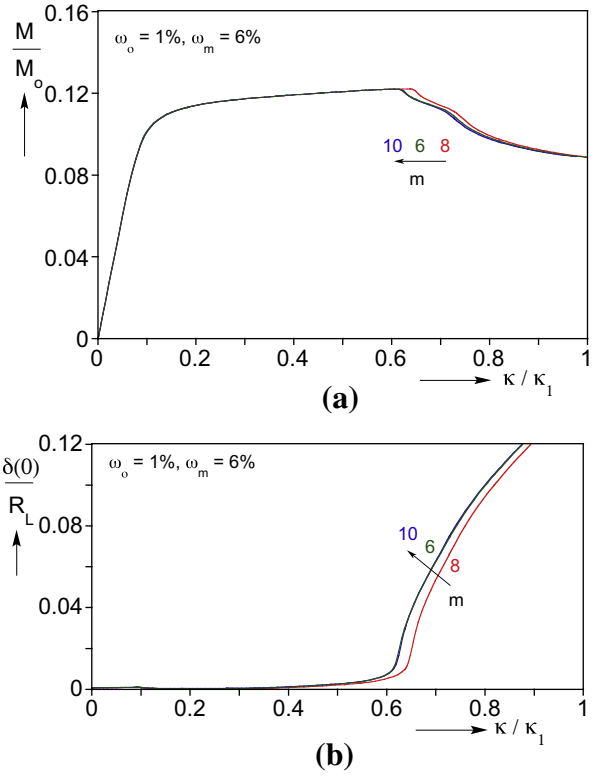

Fig. 12. Effect of circumferential wave number on liner response. (a) Moment–curvature and (b) maximum detachment-curvature responses.

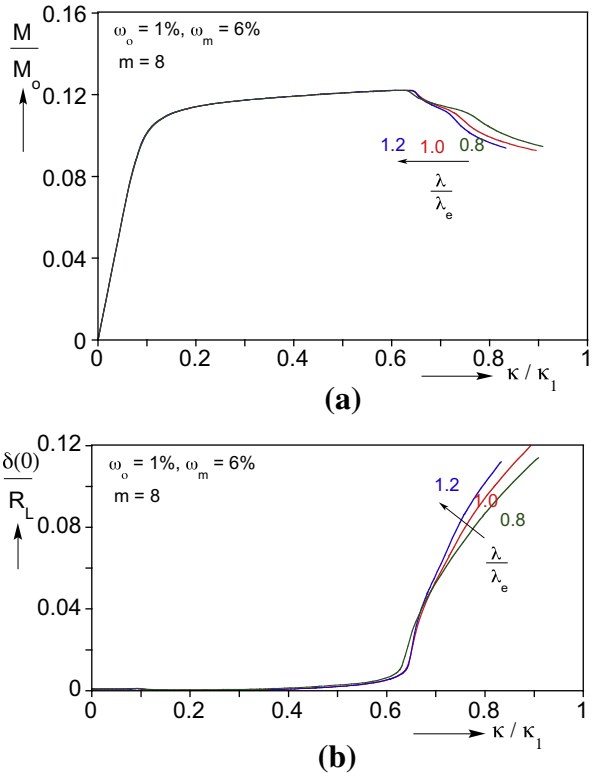

Fig. 13. Effect of axial wavelength of imperfections on liner response. (a) Moment–curvature and (b) maximum detachment-curvature responses.

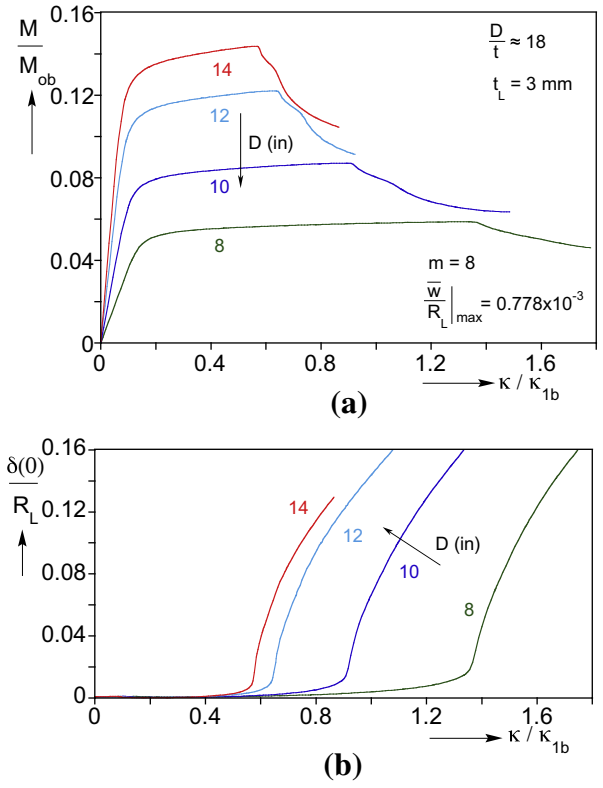

Fig. 14. Effect of pipe diameter on liner response for a constant liner wall thickness. (a) Moment–curvature and (b) maximum detachment-curvature responses.

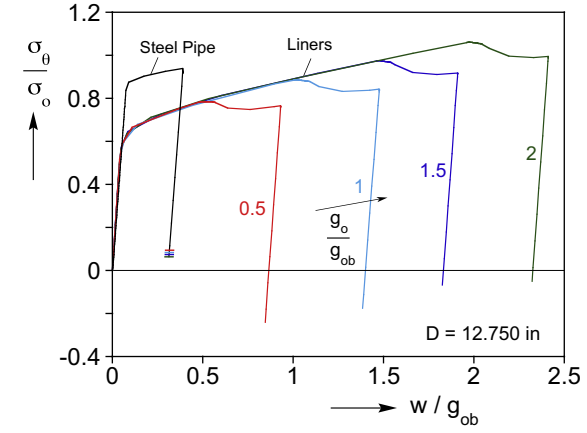

Fig. 15. Circumferential stress-displacement responses of bi-material structure during hydraulic expansion for different values of initial annular gap.

Fig. 16a shows the liner moment–curvature responses and Fig. 16b the corresponding maximum separation-curvature results. The overall behavior of the liner is similar in all cases, but clearly increasing g_o results in a decrease in the collapse curvature of the liner. The importance of this parameter on the integrity of the liner under bending is highlighted by the observation that the decrease in collapse curvature between the smallest gap used and the largest is more than 50%. This sensitivity of the liner collapse curvature to g_o indicates that, to the extent that is practically feasible, its value should be minimized. This places tighter demands on the manufacture of the two tubes for increased straightness and roundness.

It is also interesting to observe that increasing g_o has the effect of increasing the moment carried by the liner, a direct consequence of the additional strain hardening resulting from the increased expansion undergone by the liner.

4.3. Liner wall thickness

As might be expected, the wall thickness of the liner plays a decisive role on its stability under bending and deserves special attention (e.g., see Tkaczyk et al., 2011). We thus consider a 12-inch composite system like the one in Table 1 but assign the liner thickness six values between 2.0 and 4.5 mm. The annular gap is kept the same and so are the mechanical properties. The liner is assigned initial geometric imperfections as defined in Eq. (2) with the half-wavelength λ calculated for each value of t_L in accordance with Eq. (1). Each composite system is expanded in the same way. The imperfection amplitudes were chosen such that the post-expansion absolute values of the amplitudes were similar for the six cases ($\bar{w}/R_L \approx 0.778 \times 10^{-3}$). Each system was purely bent, and the calculated liner moment- and maximum detachment-curvature responses are shown in Fig. 17. Qualitatively the behavior of the composite structures is similar to that described for the base case. The results clearly show that increasing the liner thickness increases the moment carried by the liner (Fig. 17a) and simultaneously delays the onset of liner collapse. It is important to note however, that since the cost of lined pipe is significantly influenced by the material cost of the non-corrosive liner, the improvement in collapse curvature resulting from the increase in t_L demonstrated here must be weighed against the related increase to the cost of the product. It is possible that calculations like the present ones can be used to conduct a cost-performance analysis to select the optimal liner thickness for a given outer pipe diameter.

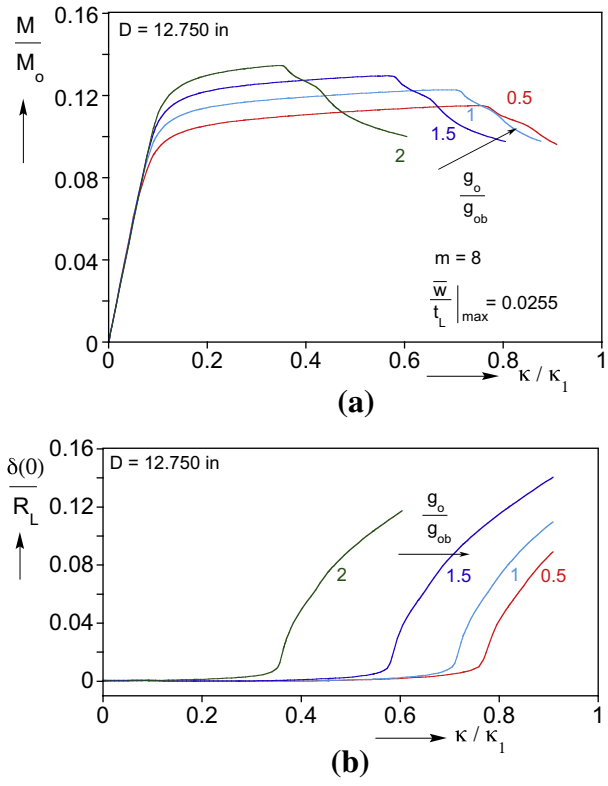

Fig. 16. Effect of initial annular gap on liner response. (a) Moment–curvature and (b) maximum detachment-curvature responses.

4.4. Bending under internal pressure

A practical method of delaying liner buckling and collapse during reeling that has been proposed by industry is to internally pressurize the pipe (e.g., Endal et al., 2008; Toguyeni and Banse, 2012; Montague et al., 2010). In essence, the section of line that is to be reeled is isolated by moveable pigs and pressurized to a few bars. Once in contact with the reel one of the pigs is moved to include an adjacent stalk, which is then pressurized and the reeling continues (Mair et al., 2013; see also Howard and Hoss, 2011).

In the way of evaluating the effectiveness of pressurization in delaying liner collapse, the 12-inch base case is now bent under increasing values of internal pressure. This is done following the initial expansion of the two-part system in accordance with the steps described in Section 2.1. Fig. 18 shows bending results for the base case and for three levels of internal pressure: 30, 50 and 100 psi (2.07, 3.45 and 6.9 bar). Qualitatively the behavior is similar to that of the unpressurized case. However, even such modest levels of internal pressure have a stabilizing effect on the liner causing a delay in its collapse. It is interesting to observe that for the imperfection used at $P = 100$ psi (6.9 bar) the liner remained stable at curvatures of $2\kappa_1$ and beyond (maximum bending strain of about 5%). A beneficial effect of the pressure is illustrated in Appendix A that shows the liner to remain in contact with the outer pipe at much larger curvature values than the unpressurized case. Although the same exercise must be repeated for the more complex bending cycle of spooling and unspooling a lined pipe on a reel, the results indicate that internal pressurization during the process may indeed make otherwise non-reelable pipe systems reelable. It is interesting to point out that previous studies have demonstrated that internal pressure can delay buckling of shells under bending (e.g., Mathon and Limam, 2006; Limam et al., 2010).

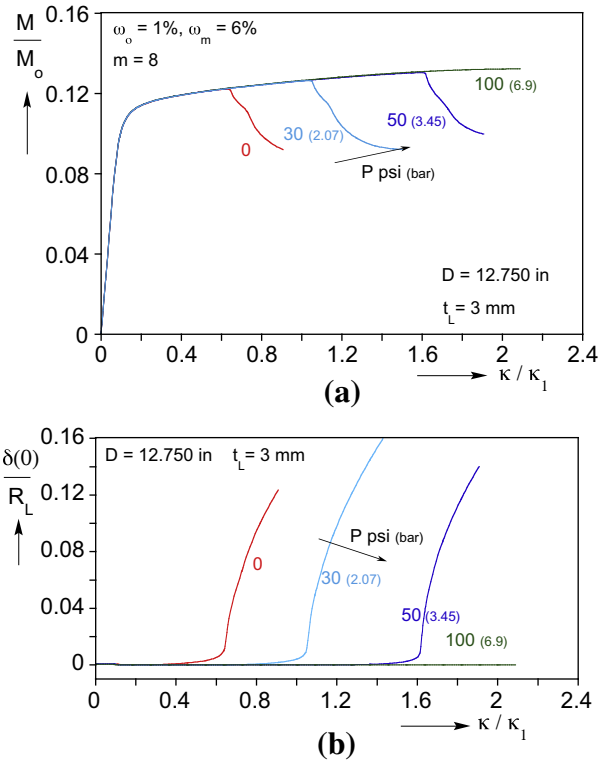

Fig. 18. Effect of internal pressure on liner response. (a) Moment–curvature and (b) maximum detachment-curvature responses.

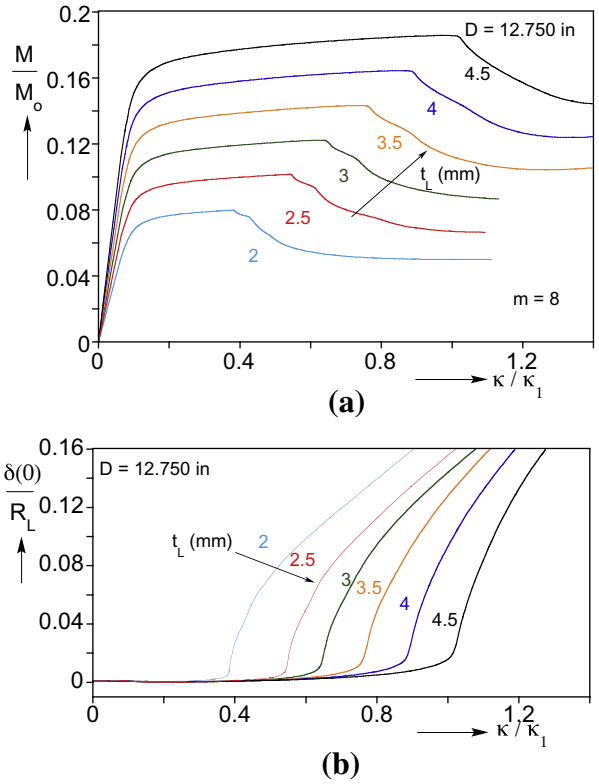

Fig. 17. Effect of liner wall thickness on its response. (a) Moment–curvature and (b) maximum detachment-curvature responses.

5. Summary and conclusions

Low-carbon steel linepipe used in offshore and other operations is often lined internally with a thin layer of corrosion resistant material in order to protect it from corrosive contents. In applications where such bi-material pipe is bent plastically, as for example in the installation of a pipeline using the reeling method, the liner can detach from the outer pipe and collapse forming large amplitude buckles that compromise the flow and generally the integrity of the structure. This paper presented a numerical framework for establishing the extent to which lined pipe can be bent before liner collapse. The models developed were used to first study the problem parametrically and then to evaluate methods for delaying the collapse of the liner.

The modeling starts by simulating the manufacture of lined pipe by mechanical expansion of the liner and the steel outer pipe. Expansion alters the mechanical properties of the two pipes and results in interference contact pressure between the two.

Pure bending of the composite structure leads to the usual Brazier ovalization of its cross section. Differential ovalization leads to gradual reduction of the contact stress between the two components and to the eventual separation of the liner from the steel tube. Without the support of the substrate, the liner sector on the compressed side in turn develops periodic wrinkles. The wrinkles initially grow stably, but as is common to shell plastic buckling problems, at some point yield to a diamond-type shell buckling mode that involves several circumferential waves. This second instability is associated with a drop in the load carried by the liner, is local in nature, and results in collapse of the liner.

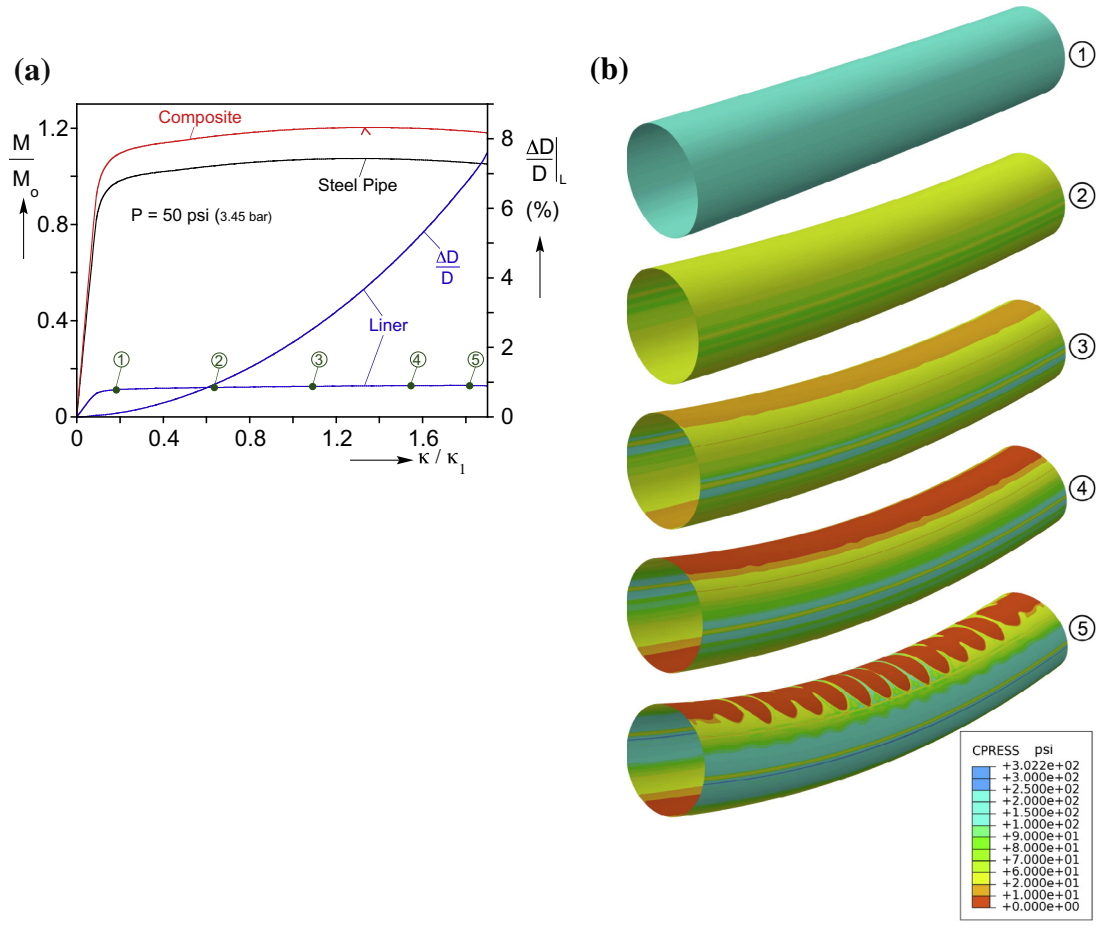

Fig. A1. (a) Base case moment- and ovalization-curvature responses. (b) Liner deformed configurations with superimposed contours of liner contact pressure; correspond to numbered bullets on liner response in (a).

The collapse curvature was found to be very sensitive to initial geometric imperfections corresponding to the two modes: that is, axisymmetric periodic wrinkling modes with wavelength 2λ, as well as to non-axisymmetric modes with m circumferential waves. This sensitivity was studied by adopting an imperfection that additively combines the two modes. Within the range of parameters considered, collapse was relatively insensitive to λ and m.

Other parameters considered include the following:

(a) In the specific manufacturing process simulated, for practical reasons, the two tubes start with an annular gap between them. It was shown that reducing this gap increases the expansion induced contact stress, which in turn has a stabilizing effect on the liner.
(b) Increasing the diameter of the composite structure reduces the collapse curvature of the liner.
(c) Increasing the wall thickness of the liner of a given system has the intuitively expected effect of delaying liner collapse. However, this benefit has to be considered vis-à-vis the resultant additional cost of the product.
(d) Bending lined pipe in the presence of relatively modest levels of internal pressure was shown to delay liner collapse. Internal pressure tends to delay separation of the liner from the outer pipe with corresponding delay in the wrinkling and non-axisymmetric buckling instabilities.

In closing, this and previous studies have clearly shown that liner buckling and collapse is very imperfection sensitive. The main sources of geometric imperfections are the internal surface roughness of the steel outer pipe and liner geometric deviations introduced during its manufacture. Efforts to quantify and, to the extent possible, reduce such imperfections should be encouraged by both manufacturers as well as users of lined pipe.

Acknowledgements

The work reported was conducted with financial support of a consortium of industrial sponsors under the project Structural Integrity of Offshore Pipelines. This support is acknowledged with thanks. The authors are also grateful to Butting management and engineers for information provided about their lined pipe product BuBi®-pipe and generally for their cooperation and help. Early results from this study appeared also in Yuan and Kyriakides, 2013.

Appendix A. Effect of internal pressure on wrinkling of perfect liner

To illustrate another aspect of the stabilizing effect of internal pressure on the liner, the 12-inch base case analyzed in Section 3.1 is bent once more but under an internal pressure of 50 psi (3.45 bar). In this calculation the composite structure has no imperfections. Fig. A1a shows the calculated moment- and ovalization-curvature responses of the two components up to a curvature of nearly 1.9 κ_1. It is noteworthy that a moment maximum develops at $\kappa = 1.33\kappa_1$. Beyond this curvature the structure is expected

to develop localized diffuse ovalization and is designated as the collapse curvature of the composite tube. In the present case collapse was avoided because of the relatively short section of tube analyzed so the analysis was continued further. Fig. A1b shows a set of corresponding liner deformed configurations with superimposed color contours that correspond to the contact pressure between the liner and the outer pipe. In configuration ① early in the bending history, the contact pressure is about 300 psi and is uniformly distributed. In configuration ② at $\kappa = 0.636\kappa_1$, the two tubes remain in contact but the contact pressure is reduced in the most stressed zones of the cross section. In configuration ③ at $\kappa = 1.09\kappa_1$, the contact pressure is very small. In configuration ④ at $\kappa = 1.54\kappa_1$, the liner has partially separated from the outer tube, and in configuration ⑤ at $\kappa = 1.82\kappa_1$ the liners has wrinkled. Comparing the present results with those of the unpressurized case in Fig. 6 we observe that in that case at a curvature $0.636\kappa_1$ the liner had already separated from the outer pipe and at $\kappa = 0.818\kappa_1$ is wrinkled. Clearly then, the main effect of the internal pressure, even at this modest level, is to delay the separation of the liner from the outer pipe. This in turn delays the onset of wrinkling and the incipient collapse.

References

Bardi, F.C., Kyriakides, S., 2006. Plastic buckling of circular tubes under axial compression. Part I Experiments. Int. J. Mech. Sci. 48, 830–841.

Bardi, F.C., Kyriakides, S., Yun, H.D., 2006. Plastic buckling of circular tubes under axial compression: Part II analysis. Int. J. Mech. Sci. 48, 842–854.

Brazier, L.G., 1927. On the flexure of thin cylindrical shells and other thin sections. Proc. R. Soc. London A116, 104–114.

Butting Brochure: Butting Bimetal-Pipes (BuBi®-pipes) (see also http://www.butting.com/mechanically_lined_pipes.html).

Corona, E., Lee, L.-H., Kyriakides, S., 2006. Yield anisotropy effects on buckling of circular tubes under bending. Int. J. Solids Struct. 43 (7099–7118), 2006.

De Koning, A.C., Nakasugi, H., Li, P., 2003. TFP and TFT back in town (Tight fit CRA lined pipe and tubing). Stainless Steel World, 53–61, Jan./Feb. 2004.

Endal, G., Levold, E., Ilstad, H., 2008. Method for laying a pipeline having an inner corrosion proof cladding. World International Property Organization, Publ. No. WO 2008/072970 A1.

Focke, E.S., 2007. Reeling of tight fit pipe. (Ph.D. thesis). Delft Technical University, ISBN 978-90-9021849-6.

Hilberink, A., 2011. Mechanical Behaviour of Lined Pipe (Ph.D. thesis). Delft Technical University, ISBN 978-94-6186-012-5.

Hilberink, A., Gresnigt, A.M., Sluys, L.J., 2010. Liner wrinkling of lined pipe under compression: a numerical and experimental investigation. In: Proc. 29th Int'l Conf. Ocean, Offshore and Arctic Eng., OMAE2010-20285, Shanghai, June 2010.

Hilberink, A., Gresnigt, A.M., Sluys, L.J., 2011. Mechanical behaviour of lined pipe during bending: numerical and experimental results compared. In: Proc. 30th Int'l Conf. Ocean, Offshore & Arctic Eng., OMAE2011-49434, Rotterdam, June 2011.

Howard, B., Hoss, J.L., 2011. Method of spooling a bi-metallic pipe. US Patent Application Publication, US 2011/0186673 A1.

Ju, G.T., Kyriakides, S., 1991. Bifurcation versus limit load instabilities of elastic-plastic tubes under bending and pressure. ASME J. Offshore Mech. Arct. Eng. 113, 43–52.

Ju, G.T., Kyriakides, S., 1992. Bifurcation and localization instabilities in cylindrical shells under bending: part II Predictions. Int. J. Solids Struct. 29, 1143–1171.

Koiter, W.T., 1963. The effect of axisymmetric imperfections on the buckling of cylindrical shells under axial compression. Proc. Kon. Ned. Ah. Wet B66, 265–279.

Kyriakides, S., Corona, E., 2007. Mechanics of Offshore Pipelines: Volume 1 Buckling and Collapse. Elsevier, Oxford, UK and Burlington, Massachusetts.

Kyriakides, S., Bardi, F.C., Paquette, J.A., 2005. Wrinkling of circular tubes under axial compression: effect of anisotropy. ASME J. Appl. Mech. 72, 301–305.

Limam, A., Lee, L.-H., Corona, E., Kyriakides, S., 2010. Inelastic wrinkling and collapse of tubes under combined bending and internal pressure. Int. J. Mech. Sci. 52, 637–647.

Mair, J.A., Schuller, T., Holler, G., Henneicke, F., Banse, J., 2013. Reeling and unreeling and internally clad pipeline. US Patent Application Publication, US 2013/0034390 A1.

Mathon, C., Limam, A., 2006. Experimental collapse of thin cylindrical shells submitted to internal pressure and pure bending. Thin Wall. Struct. 44, 39–50.

Montague, P., 2004. Production of clad pipes. Int'l Application, Patent Cooperation Treaty, Pub. No. WO 2004/103603 A1, 02-12-2004.

Montague, P., Walker, A., Wilmot, D., 2010. Test on CRA lined pipe for use in high temperature flowlines. In: Proc. Offshore Pipeline Tech. Conf., Amsterdam, Netherlands, Feb. 24–25, 2010.

Peek, R., Hilberink, A., 2013. Axisymmetric wrinkling of snug-fit lined pipe. Int. J. Solids Struct. 50, 1067–1077.

Rommerskirchen, I., Schuller, T., Blachinger, B., Schafer, K., 2003. New liner materials used in BuBi-pipes. In: Proc. Stainless Steel World. KCI Publishing BV, pp. 49–53, ISBN 9073168201.

Shrivastava, S., 2010. Elastic/plastic bifurcation buckling of core-filled circular and square tubular columns. In: Proc. 16th US National Congress of Theoretical and Applied Mechanics. State College, PA, USA, USNCTAM2010-524.

Tkaczyk, T., Pepin, A., Denniel, S., 2011. Integrity of mechanically lined pipes subjected to multi-cycle plastic bending. In: Proc. 30th Int'l Conf. Ocean, Offshore & Arctic Eng., OMAE2011-49270, Rotterdam, June 2011.

Toguyeni, G., Banse, J., 2012. Mechanically lined pipe: installation by reel-lay. In: Proc. Offshore Techn. Conf., OTC 23096, Houston, TX, April 30–May 3.

Tvergaard, V., 1983. On the transition from a diamond mode to an axisymmetric mode of collapse in cylindrical shells. Int. J. Solids Struct. 19, 845–856.

Vasilikis, D., Karamanos, S.A., 2010. Buckling of double-wall elastic tubes under bending. In: 9th HSTAM Int'l Congress on Mechanics, Limassol, Cyprus, July 2010.

Vasilikis, D., Karamanos, S.A., 2012. Mechanical behavior and wrinkling of lined pipes. Int. J. Solids Struct. 49, 3432–3446.

Wilmot, D., Montague, P., 2011. The suitability of CRA lined pipes for flowlines susceptible to lateral buckling. In: SUT Global Pipeline Buckling Symposium, Perth, Australia, Feb. 23–24, 2011.

Yuan, L., Kyriakides, S., 2013. Wrinkling of lined pipe under bending. In: Proc. 32nd Int'l Conf. Ocean, Offshore & Arctic Eng., OMAE2013-11139, Nantes, France, June 2013.

Yun, H.D., Kyriakides, S., 1990. On the beam and shell modes of buckling of buried pipelines. Soil. Dyn. Earthq. Eng. 9, 179–193.